where h is the nondimensional pivot position and D' can be obtained by replacing M_∞ by $M_\infty/\cos\varphi$ in D of Ref. 2. Also, allowance has to be made for a different notation, e.g., the wedge half-angle is δ, whereas in Ref. 2 it is θ.

For a plane ogive (the nonplanar wedge of Ref. 2),

$$M_p = \text{right side of Eq. (6)} + \frac{U_\infty \cos(\delta-\theta)\,(dy'/dx')}{a_\infty \cos\varphi} \tag{9}$$

where dy'/dx' is the slope of the upper surface.

The derivatives for an ogive are

$$-Cm_\theta = \frac{(\gamma+1)}{2M_\infty^2\cos^2\delta}(I_1' + I_2' + I_3') \tag{10a}$$

$$-Cm_q = \frac{(\gamma+1)}{2M_\infty\cos^3\delta\cos\varphi}(J_1' + J_2' + J_3') \tag{10b}$$

where I_1', J_1', etc. can be obtained from I_1, J_1, etc. of Ref. 2 in the same way as D'.

Discussion and Results

For a steady wedge, the present similitude applies in a plane normal to the shock, is exact, and is restricted to $M_\infty > 1$. The similitude of Ref. 2 applies in a plane normal to the wedge surface, has an error of $\mathcal{O}(\varphi^2)$, and is restricted to $M_\infty \geq 5$. For a quasiwedge or an oscillating wedge, another constraint in addition to the Mach number restriction is necessary: $E \leq 0.3$ for the present similitude and $M_2 \geq 2.5$ for the similitude of Ref. 2 (see also Ref. 4).

In the hypersonic domain, both similitudes are valid and the order-of-magnitude analysis indicates the existance of the same error for both since E, $\Phi = 0(\varphi)$. Also since $\varphi \ll 1$, the cos φ factor of Eq. (5) makes a small difference of $\mathcal{O}(\varphi^2)$, which is within the error of the similitude of Ref. 2. However in the context of the present similitude, the solution for quasiwedge or oscillating wedge is a small departure from an exact solution and, hence, is likely to be an improvment on Ref. 2.

Cm_θ is concerned with a steady rotation in pitch; hence, the present method is exact and gives identical results with Ref. 6 (Fig. 2). Cm_q shows a comparable trend with $Cm_{\dot\theta}$ (Fig. 2); note that there is no other theory for Cm_q. The effect of convexity in the plane ogives is to decrease the stiffness and shift the damping minima forward (Fig. 3).

References

[1]Ghosh, K., "A New Similitude for Aerofoils in Hypersonic Flow," *Proceedings of 6th Canadian Congress of Applied Mechanics*, May 1977, pp. 685-686.

[2]Ghosh, K. and Mistry, B. K., "Large Incidence Hypersonic Similitude and Oscillating Nonplanar Wedges," *AIAA Journal*, Vol. 18, Aug. 1980, pp. 1004-1006.

[3]Ghosh, K. "Hypersonic Large-Deflection Similitude for Oscillating Delta Wings," *The Aeronautical Journal*, Oct. 1984, pp. 357-361.

[4]Ghosh, K. "Hypersonic Large-Deflection Similitude for Quasi-Wedges and Quasi-Cones," *The Aeronautical Journal*, March 1984, pp. 70-76 and "Correction," Aug./Sept. 1984, p. 328.

[5]Sedov, L. I., *Similarity and Dimensional Methods in Mechanics*, Gostekhizdat, Moscow 1943; English translation by M. Hott, Academic Press, New York, 1959.

[6]Hui, W. H., Stability of Oscillating Wedges and Caret Wings in Hypersonic and Supersonic Flows," *AIAA Journal*, Vol. 7, Aug. 1969, pp. 1524-1530.

[7]Ghosh, K., "Unified Similitude for Wedge and Cone with Attached Shock," *Proceedings of 9th Canadian Congress of Applied Mechanics*, May 1983, pp. 533-544.

Shock/Turbulent Boundary-Layer Interaction with Wall Function Boundary Conditions

S. K. Saxena* and R. C. Mehta*

Vikram Sarabhai Space Centre, Trivandrum, India

Introduction

In recent years, advances in the efficiency of numerical methods[1,2] for the computation of compressible viscous flows have substantially reduced computing times. The problem of the computation of turbulent flows, however, remains a major challenge. One difficulty is due to the fact that integration of the Reynolds-averaged Navier-Stokes equations up to the wall with zero slip boundary conditions needs fine mesh spacing in the vicinity of the wall in order to capture rapid variation of the flowfield in that region.

Launder and Spalding[3] and Chieng and Launder[4] have demonstrated that the wall function approach eliminates the requirement of very fine mesh close to the wall. Their treatment was, however, limited to incompressible flows. Recently, Rubesin and Viegas[5] have extended the wall function approach to complex compressible flows. In all these attempts, wall functions were used with two equation models of turbulence, and the effect of adverse pressure gradient was not taken into account in the law of the wall.

The present Note describes a formulation of wall function approach to boundary conditions in which a modified law of the wall is employed in the regions where adverse pressure gradient exists. Its effectiveness is demonstrated by application to the problem of numerical simulation of shock/turbulent boundary-layer interaction with an adiabatic wall and Cebeci-Smith model of turbulence. Substantial saving in computation time and memory requirements is achieved without significantly affecting the accuracy of the solution. The formulation can be easily extended to treat a nonadiabatic wall.

Analysis

The differential equations used to describe the mean flow for this study are the time-dependent, Reynolds-averaged Navier-Stokes equations written in conservation form and Cartesian coordinates for plane flow of a compressible fluid.

The present wall function approach is depicted in Fig. 1. The first mesh volume off the surface is between $y=0$ and $y=y_e$ such that its center (2) is located well into the fully turbulent region ($y^+ \geq 50$). This volume is only partly filled with fully turbulent flow and is partially composed of the viscous sublayer with its edge at $y=y_v$. The second mesh volume is between $y=y_e$ and $y=y_f$ and is centered at point (3). Point (1) is the mirror image of point (2) and is the center of the fictitious boundary cell. All these mesh volumes described above are used in the numerical computation. However, in the wall function model, only the first mesh volume off the surface is used.

The incompressible law of the wall is given by

$$u^+ = (1/K)\ell n(y^+) + B \tag{1}$$

where

$$K = 0.41 \text{ and } B = 5$$

$$u^+ = u/u_\tau,\ y^+ = yu_\tau/v_\omega,\ v_\omega = \mu_\omega/\rho_\omega, \text{ and } u_\tau = (\tau_\omega/\rho_\omega)^{1/2}$$

Received July 25, 1985; revision received Sept. 16, 1985.

*Engineer, Aerodynamics Division.

However, in the regions where adverse pressure gradient exists, the following law of the wall[6] has been employed

$$u^+ = \left(\frac{1}{k^*}\right)\left[3(t-t_s) + \ell n\left(\frac{t_{s+1}}{t_{s-1}}\,\frac{t-1}{t+1}\right)\right] \tag{2}$$

where

$$t = (1+2\tau^+/3)^{1/2}$$

$$t_s = (1+0.074\alpha)^{1/2}$$

$$\tau^+ = 1+\eta$$

$$\eta = \alpha y^+$$

$$\alpha = \nu_\omega \rho_\omega^{1/2}(dp/dx)/\tau_\omega^{3/2}$$

$$k^* = (0.4+0.6\alpha)/(1+\alpha)$$

At high Mach number ($M_\infty > 4$), where the compressibility effects in turbulence becomes significant, the law of the wall can be extended to compressible flow through the use of the van Driest transformation.[7] The effective u^+ then becomes

$$u^+ = \frac{1}{u_\tau}\int_0^u (\rho/\rho_\omega)^{1/2}\,du \tag{3}$$

It is a reasonably good approximation to take wall pressure p_w as equal to pressure at point (2), i.e.,

$$p_w = p_2 \tag{4}$$

The knowledge of wall temperature T_w is required to evaluate ρ_ω and ν_ω. Under high-speed conditions, T_w cannot be set equal to T_2, even for an adiabatic surface. This is due to the fact that the first mesh volume off the surface is not entirely filled with fully turbulent flow but is partially composed of the viscous sublayer, which is reflected in the complex variations of the dependent variables across the mesh volume. In such a situation, T_w is found by considering that the heat flux between the surface and the first mesh point y_2 to behave as in Couette flow, namely,

$$\dot{q}_y - u\tau_{xy} = \dot{q}_\omega \tag{5}$$

Equation (5) can be integrated without difficulty for a nonadiabatic wall.[5] Present work considers that an adiabatic wall and Eq. (5) can be integrated directly to yield

$$T = T_w - (Pr/2C_p)u^2 \tag{6}$$

for $u < u_v$ in the viscous sublayer and

$$T = T_w - (Pr_t/2C_p)u^2 + [(Pr_t - Pr)/2C_p]u_v^2 \tag{7}$$

in the fully turbulent portion of the boundary layer. The laminar and turbulent Prandtl number, Pr and Pr_t, are taken as 0.72 and 0.9, respectively.

Since the velocity u and temperature T are evaluated at point (2) as part of the dependent field variables, Eq. (7) can be used to compute wall temperature, once u_v is found. The

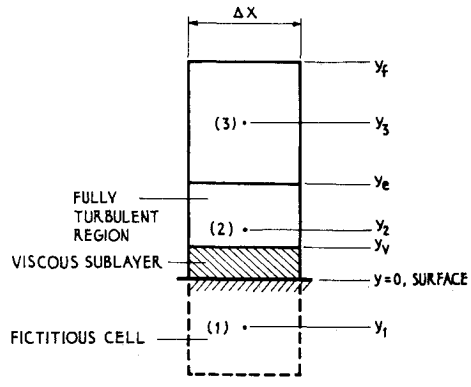

Fig. 1 Near-wall physical model.

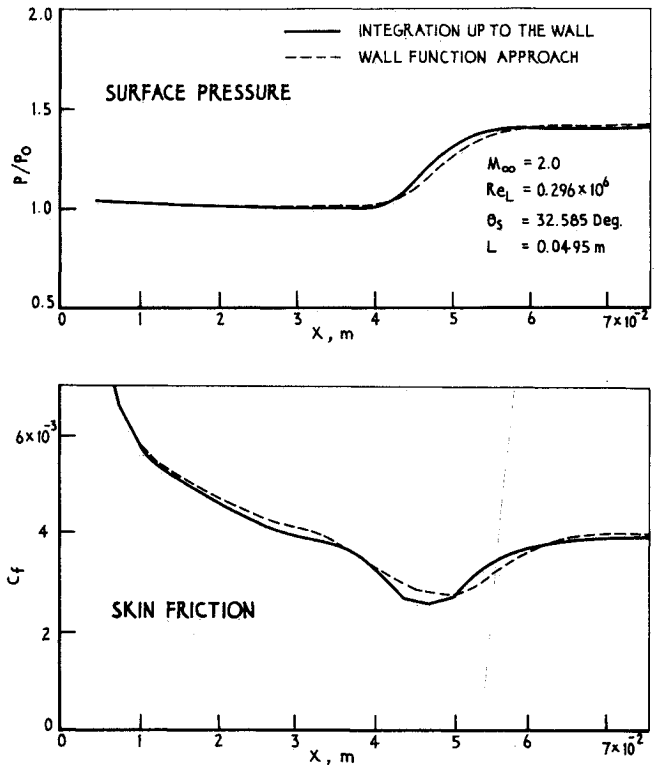

Fig. 2 Wall pressure and skin friction distribution.

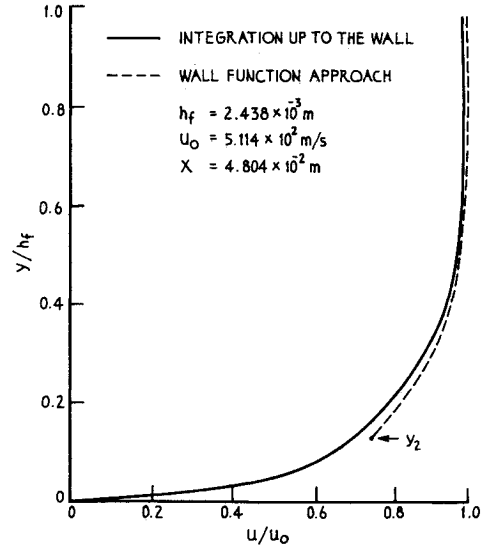

Fig. 3 Turbulent velocity profile.

velocity u_v occurs at the viscous sublayer edge y_v, which is assumed to be located by

$$y^+ = u_\tau y_v / \nu_\omega = 10 \tag{8}$$

It is further assumed that the following law holds good in the viscous sublayer $u^+ = y^+$, which gives

$$u_v = \tau_\omega y_v / \mu_\omega \tag{9}$$

Equations (1), (2), (4), and (7-9) are solved, together with the perfect gas law and the Sutherland viscosity equation, to yield y_v, u_v, T_w, ρ_ω, μ_w, and τ_w.

Results and Discussion

The Reynolds-averaged Navier-Stokes equations are solved using MacCormack's implicit scheme[1] to simulate numerically shock/turbulent boundary-layer interaction. The results are obtained by integrating to the wall (ITW), as well as with wall function approach (WFA), for the following test case: $M_\infty = 2.0$, $Re_L = 0.296 \times 10^6$, and $\theta_s = 32.585$ deg (incident shock angle with the X direction). The wall is considered adiabatic. In the present test case, which is the same as the one considered by MacCormack,[8] the boundary layer does not separate as a result of interaction with the shock.

In ITW, the mesh required 32×32 grid points with 16 points in the boundary layer. The WFA required only 32×26 grid points with 10 grid points in the boundary layer—about 20% reduction in the number of grid points compared with the first case. In both cases, the starting CFL number is as high as 10, which is gradually reduced as the convergence is approached to avoid possible steady-state solution dependence on time increment Δt.[9]

The wall pressure and skin friction obtained with ITW and WFA are presented in Fig. 2. The corresponding velocity profile at $X = 4.804 \times 10^{-2}$ m are compared in Fig. 3. The figures reveal that the results obtained with the wall function approach are in good agreement with those obtained with integration to the wall.

The results of this study were obtained on a CDC Cyber 170/730 computer. It took about 25 min of CPU time to obtain converged solution with integration to the wall, while the wall function approach required about 15 min of CPU time.

In conclusion, the wall function formulation presented has been shown to result in substantial saving in computation time and storage requirements compared with integration to the wall, without significantly affecting the accuracy of the solution.

References

[1]MacCormack, R. W., "A Numerical Method for Solving the Equations of Compressible Viscous Flow," *AIAA Journal*, Vol. 20, Sept. 1982, pp. 1275-1281.

[2]Beam, R. M. and Warming, R. F., "An Implicit Factored Scheme for the Compressible Navier-Stokes Equations," *AIAA Journal*, Vol. 16, April 1978, pp. 393-402.

[3]Launder, B. E. and Spalding, D. B., "The Numerical Computation of Turbulent Flows," *Computer Methods in Applied Mechanics and Engineering*, Vol. 3, 1974, pp. 269-289.

[4]Chieng, C. C. and Launder, B. E., "On the Calculation of Turbulent Heat Transfer Downstream from an Abrupt Pipe Expansion," *Numerical Heat Transfer*, Vol. 3, 1980, pp. 189-207.

[5]Rubesin, M. W. and Viegas, J. R., "A Critical Examination of the Use of Wall Functions as Boundary Conditions in Aerodynamic Calculations," presented at Third Symposium on Numerical and Physical Aspects of Aerodynamic Flows, California State University, Long Beach, Jan. 20-24, 1985.

[6]Nakayama, A. and Koyama, H., "A Wall Law for Turbulent Boundary Layers in Adverse Pressure Gradients," *AIAA Journal*, Vol. 22, Oct. 1984, pp. 1386-1389.

[7]Hopkins, E. J., Keener, E. R., Polek, T. E., and Dwyer, H. A., "Hypersonic Turbulent Skin Friction and Boundary Layer Profiles Measured on Nonadiabatic Flat Plates," *AIAA Journal*, Vol. 10, Jan. 1972, pp. 40-48.

[8]MacCormack, R. W., "Numerical Methods for Compressible Viscous Flows," presented at the Workshop-cum-Seminar on Computational Fluid Dynamics, Vikram Sarabhai Space Centre, Trivandrum, India, Dec. 14-21, 1981.

[9]Gupta, R. N., Gnoffo, P. A., and MacCormack, R. W., "A Viscous Shock-Layer Flowfield Analysis by an Explicit-Implicit Method," NASA TM 84668, May 1983.

Nonuniform Nozzle Flow Effects on Base Pressure at Supersonic Flight Speeds

A. L. Addy,* J. C. Dutton,† and V. A. Amatucci‡
University of Illinois at Urbana-Champaign
Urbana, Illinois

Introduction

ANALYTICAL investigations of missile base flow during powered flight at supersonic speeds are principally based on one of the computer implementations of the Chapman-Korst component flow model.[1-3] To improve agreement with experiments, empirical modifications of this analysis are usually used based on small-scale experimental results. In the component model, the propulsive nozzle is generally represented as an ideal nozzle which produces either uniform or conical flow at the nozzle exit. However, many of the small-scale experiments and full-scale prototypes employ nozzle geometries which have a small radius of curvature of the throat wall, a conical expansion section with a relatively large divergence angle, and/or a truncated expansion section. These nozzles would be expected to produce nonuniform and nonconical flow at the exit, thereby affecting the plume expansion into the base region. These effects have often been hypothesized as some of the possible causes of the disagreement between the component model predictions and experimental results, although no systematic investigation of their significance on base flow has been reported. The purpose of this paper is to present parametric results of nonuniform nozzle flow effects on base pressure for typical conical nozzle geometries in order to determine their expected magnitudes and to test the hypothesis stated.

Method of Analysis

The missile base configuration under consideration is shown in Fig. 1. The internal nozzle flow expands through a conical nozzle with a circular arc throat to supersonic conditions at the exit. The nozzle geometry is completely specified by the dimensionless throat wall radius of curvature R_{CW}/R_T, by the nozzle exit radius ratio R_I/R_T, and by the divergence half-angle β_I. The external freestream flow is also assumed to be supersonic, and for the cylindrical afterbody considered, the only pertinent geometric variable is the base radius ratio R_I/R_E. The freestream and nozzle flows separate at the base and expand or compress, as the case may be, to a common base pressure P_B. A recompression

Received July 29, 1985.

*Professor and Associate Head, Department of Mechanical and Industrial Engineering. Associate Fellow AIAA.

†Associate Professor, Department of Mechanical and Industrial Engineering. Member AIAA.

‡Graduate Research Assistant, Department of Mechanical and Industrial Engineering. Student Member AIAA.